

1

Supporting Information

2 **PKC δ -mediated SGLT1 upregulation confers the acquired resistance of NSCLC**
3 **to EGFR TKIs**

4 Chia-Hung Chen, Bo-Wei Wang, Yu-Chun Hsiao, Chun-Yi Wu, Fang-Ju Cheng,
5 Te-Chun Hsia, Chih-Yi Chen, Yihua Wang, Zhang Weihua, Ruey-Hwang Chou,
6 Chih-Hsin Tang, Yun-Ju Chen, Ya-Ling Wei, Jennifer L. Hsu, Chih-Yen Tu,
7 Mien-Chie Hung, Wei-Chien Huang

8 This file includes:

9 Materials and Methods

10 Supplementary Fig 1~8

11 Supplementary Table 1

12 **Materials and Methods**

13 ***Reagents and plasmids***

14 Erlotinib (#S1023) and gefitinib (#S5098) were obtained from Selleckchem (Houston,
15 TX, USA). SGLT inhibitors phlorizin (# 60-81-1) and LX4211 (# HY-15516) were
16 obtained from PubChem (Bethesda, MD, USA) and MedChem Express (Monmouth
17 Junction, NJ, USA), respectively. D-glucose (#15023-021) was purchased from
18 Thermo Fisher Scientific (Waltham, MA, USA). 2-Deoxy-D-glucose (2-DG)
19 (#MER-25972), 3-methyladenine (3-MA) (#SI-M9281), chloroquine (CQ) (#
20 SI-C6628), propidium iodide (PI) (#P4170), and oligomycin (# 75351) were
21 purchased from Sigma-Aldrich. MG-132 (# 10012628), GO6983 (# 13311),
22 sotrastaurin (#16726), staurosporine (#81590), and everolimus (#11597) were
23 purchased from Cayman Chemical (Ann Arbor, Michigan, USA). HBDDE
24 (#sc-202174) was obtained from Santa Cruz Biotechnology.
25 pLKO-shSGLT1#1(TRCN0000043590), pLKO-shSGLT1#2 (TRCN0000043592),
26 pCMV-ΔR8.91, and pMD.G were purchased from the National RNAi Core Facility of
27 Academia Sinica (Taipei, Taiwan).

28 The rabbit polyclonal antibodies specific for SGLT1 was generated from LTK
29 BioLaboratories (Taoyuan, Taiwan). The rabbit polyclonal antibodies against EGFR
30 (#sc-03; RRID:AB_631420), HER2 (Neu) (#sc-393712; RRID:AB_2810840), HER3
31 (#sc-7390; RRID:AB_2262346), HER4 (#sc-283; RRID:AB_2231308), Glut1
32 (#sc-7903; RRID:AB_2190936) were purchased from Santa Cruz Biotechnology
33 (Dallas, Texas, USA). The rabbit polyclonal antibodies specific for PARP (#9542;
34 RRID:AB_2160739), cleaved PARP (#5625; RRID:AB_10699459), phospho-EGFR
35 S1046/47 (#2238; RRID:AB_331129), phospho-EGFR T669 (#3056;
36 RRID:AB_1264152), phospho-EGFR T678 (#14343; RRID:AB_2798457),

37 phospho-PKC δ S643/676 (#9376; RRID:AB_2168834), phospho-AMPK T172
38 (#2531; RRID:AB_330330), phospho-mTOR S2448 (#2971; RRID:AB_330970),
39 mTOR (#2983; RRID:AB_2105622) and caspase 3 (#9662; RRID:AB_331439) were
40 from Cell Signaling Technology (Danvers, MA, USA). LC3 (#NB100-2220SS;
41 RRID:AB_791015) antibody was acquired from Novus Biologicals (Centennial CO,
42 USA). Rabbit polyclonal antibodies specific for PKC δ (#ab182126) and
43 phospho-PKC δ T505 (# ab60992; RRID:AB_944848) were obtained from Abcam
44 (Cambridge, United Kingdom, England). Mouse polyclonal antibody specific for
45 phospho-EGFR Y1068 (#2236; RRID:AB_331792) was purchased from Cell
46 Signaling Technology. Mouse polyclonal antibody specific for Glut3 (sc-74497;
47 RRID:AB_1124974) was acquired from Santa Cruz Biotechnology. The specific
48 rabbit polyclonal antibodies of IHC staining for SGLT1 (#ab14685;
49 RRID:AB_301410) and phospho-EGFR T678 (#ab194733) were purchased from
50 Abcam. Goat polyclonal antibody specific of SGLT2 (#sc-47402; RRID:AB_2189561)
51 was obtained from Santa Cruz Biotechnology. Actin (#A2228; RRID:AB_476697)
52 and Tubulin (#T5168; RRID:AB_477579) were acquired from Sigma-Aldrich (St.
53 Louis, Missouri, USA). HA (#11583816001; RRID:AB_514505) and Ki67
54 (#RM-9106; RRID:AB_2341197) were purchased from Roche (Basel, Switzerland)
55 and Thermo Fisher Scientific (Waltham, MA, USA), respectively.

56

57 ***Cell culture and establishment of erlotinib-resistant (ER) clones***

58 Human lung cancer H322 (CRL-5806; RRID:CVCL_1556), H292 (CRL1848;
59 RRID:CVCL_0455), A549/Luc, and HCC827 (CRL-2868; RRID:CVCL_2063) cell
60 lines and their erlotinib-resistant (ER) derivatives were cultured in RPMI 1640
61 medium supplemented with 10% FBS, 100 U/mL penicillin, and 100 mg/mL

62 streptomycin, with 10 mM HEPES. All cancer cell lines were maintained in a
63 humidified 5% CO₂ incubator at 37 °C. The ER clones of various lung cancer cell
64 lines were established from the parental cells by chronic treatment with gradually
65 increasing concentrations (up to 1µM) of erlotinib.

66

67 ***Cell counting and cell viability assays***

68 Cell viability was carried out in WST-1 colorimetric assays. Briefly, cells seeded in
69 96-well plates were pretreated with indicated inhibitors or infected with viral shRNA
70 for 24 or 72 hrs followed by the incubation with 10µl/well of WST-1 (Roche, Basel,
71 Switzerland) reagent to the cells already cultured in 100µl/ well (1:10 final dilution)
72 for 1 hr. The relative number of cells was determined by measuring the absorbance at
73 450 nm.

74

75 ***Clonogenic formation assay***

76 Cells (1×10^4 cells/well) in 12-well plates were grown in the presence of different
77 concentrations of glucose or the indicated inhibitors for 14 days. The colonies were
78 fixed and stained with 30% ethanol containing 1% crystal violet for 30 mins, and then
79 were washed with ddH₂O.

80

81 ***Autophagosome formation assay***

82 Cells seeded in 6-well plates were cultured with different glucose concentrations for
83 24 hr and were then stained with Cyto-ID[®] autophagy green dye (Enzo Lifesciences,
84 Farmingdale, NY, USA) at 37 °C for 1 hr. Cells were washed with PBS three times
85 and then fixed with 4% formaldehyde at room temperature for 20 min. The signal of
86 autophagosome was detected by ECHO Revolve (San Diego, CA, USA) or measured

87 in BD FACSCalibur.

88

89 ***Cell cycle analysis***

90 Cell seeded in 6-well plates were cultured with different glucose concentrations or
91 treated with various inhibitors for 24 hr and fixed with ice-cold 70 % ethanol
92 overnight at -20 °C. The cells were spun down and washed with PBS twice, then
93 were stained with propidium iodide (PI) solution (1ml mix of 200 µg/ml RNase and
94 50 µg/ml PI in PBS) at 37 °C for 30 min with the protection from light. The
95 subpopulation of subG1 was measured in BD FACSCalibur (BD Biosciences, San
96 Jose, CA, USA).

97

98 ***Immunoprecipitation (IP) and Western blot (WB) analysis***

99 Total lysates were prepared with lysis buffer (4 M NaCl, 1 M Tris, pH8.0), 10% SDS,
100 Triton X-100, 10% sodium deoxycholate, 0.5 M EDTA), briefly sonicated, and then
101 centrifugated at 15,000 rpm for 20 min at 4 °C followed by the collection of
102 supernatants. For immunoprecipitation, one mg of total lysate incubated with primary
103 antibody for overnight followed the incubation with protein A/G beads for 4 hours at
104 4 °C. The immunoprecipitates were washed with IP buffer (1 M HEPES, 1 M KCl, 1
105 M MgCl₂, 5 M NaCl) and eluted with sample dye. Total lysate or immunoprecipitates
106 were subjected to protein separation in 8% or 12% of SDS-PAGE followed by protein
107 transfer to polyvinyl difluoride (PVDF) or nitrocellulose (NC) membranes. The
108 membranes were blocked with 5% milk for 1 hr at room temperature and incubated
109 with primary antibodies at 4 °C overnight followed by the incubation with secondary
110 antibodies in 5% milk for 1 hr at room temperature. The protein amount was
111 developed with enhanced chemiluminescence (Bio-Rad Laboratories, Hercules, CA,

112 USA) reagent and detected in a chemiluminescence system.

113

114 ***Measurement of extracellular acidification rate (ECAR)***

115 The ECAR in lung cancer cells and their ER clones were assessed by using a

116 Seahorse XF[®]24 Analyzer (Agilent Technologies Inc., Santa Clara, CA, USA).

117 Assays were performed according to the manufacturer's instructions. In brief, cells

118 (2.5×10^4 cells/well) in 24-well XF microplate (Seahorse Biosciences, VIC, Australia)

119 were cultured in glucose-free seahorse XF assay medium. Specific inhibitors,

120 different glucose concentrations, and uncouplers were prepared in XF assay media

121 following the experiment's design for sequential addition at the appropriate final

122 concentrations (10 mM glucose, 1 μ M oligomycin, and 50 mM 2-DG). The data were

123 normalized with cell numbers.

124

125 ***2-[N-(7-Nitrobenz-2-oxa-1,3-diazol-4-yl) amino]-2-deoxy-D-glucose (2-NBDG)***

126 ***uptake assay***

127 Cells seeded in 6 well plates were pretreated with the indicated inhibitors for 3 days

128 followed by the incubation with glucose-free media for 4 hr and 2-NBDG (100

129 μ M/mL; Cayman, Ann Arbor, MI, USA) in PBS for 20 min at 37 °C. The uptake of

130 2-NBDG was detected by ECHO Revolve or measured in BD FACSCalibur.

131

132 ***[14C]- α -methyl-D-glucopyranoside (α MDG) uptake assay***

133 The active glucose uptake ability of cells was determined by measuring the uptake of

134 α -MDG (PerkinElmer, MA, USA), which is a specific substrate for SGLT. Cells

135 seeded in a 12-well plate were cultured with different glucose concentrations or

136 infected with SGLT1 shRNA. After washed with PBS once, the cells were incubated

137 with Krebs–Ringer–Henseleit (KRH; 120 mM NaCl, 4.7 mM KCl, 1.2 mM MgCl₂,
138 2.2 mM CaCl₂, and 10 mM HEPES, pH 7.4 [with Tris]) solution containing
139 [¹⁴C]-αMDG (0.1 μCi/ml) for 40 min. Following wash with PBS three times, cells
140 were lysed by 1% Triton and added 2 ml scintillation solution. Then the uptake of
141 [¹⁴C]-αMDG was counted and presented as counts per minute (CPM) value in
142 Beckman LS6000 Scintillation Counter (GMI, Ramsey, MN, USA), and the data were
143 normalized with the protein amounts.

144

145 ***2-[¹⁸F]-2-deoxy-D-glucose (FDG) uptake assay***

146 Cells seeded in a 6-well plate were treated with phlorizin under low glucose
147 concentration condition. After washed with PBS twice, the cells were incubated with
148 radioactivity-containing ¹⁸F-FDG (1μCi/mL) under glucose-free condition for 30 min.
149 Following wash with PBS for two times, the uptake of ¹⁸F-FDG was measured in
150 PerkinElmer 2470 Automatic gamma counter. (PerkinElmer Inc., MA, USA) and
151 presented as counts per minute (CPM) value. The data was normalized with cell
152 numbers.

153

154 ***Human NSCLC clinical specimens***

155 The acquisition of tumor specimens from NSCLC patients treated with EGFR TKIs
156 were approved by the Ethics Review Board of China Medical University Hospital
157 (DMR101-IRB1-120). Informed written consent was obtained from patients. The
158 tissues were fixed in 10% formalin and embedded in paraffin, and 5μm tissue slides
159 were prepared for IHC staining.

160

161 ***Immunohistochemistry Staining***

162 Five-micrometer thick paraffin wax mouse-tissue sections were dewaxing by xylene
163 and rehydrated by different concentrations of ethanol. These mouse-tissue sections
164 were incubated with the indicated antibodies overnight and then stained with polymer
165 HRP-conjugated secondary antibodies for 30 min followed by reaction with
166 diaminobenzidine (DAB; Leica, Wetzlar, Germany) for 30 sec or 1 min. These slides
167 were counterstained with hematoxylin. According to the H-score system, the
168 immune-intensity of tumor tissue was scored by calculating the percentage of positive
169 cells at different staining intensity levels, and the final score is ranked from 0 to 300.
170 The score of SGLT1 level over than 200 was defined as high expression.

171

172 ***Xenograft tumor growth assay***

173 Animal experiments were performed following a protocol approved by the
174 Institutional Animal Care and Use Committee of China Medical University and
175 Hospital (No. 102-40-N). H292 cells (1×10^6 cells/mouse) were subcutaneously
176 injected into the female severe combined immunodeficient (SCID) mice at 4 weeks of
177 age, and the tumor size was measured with calipers once per week. Once the tumor
178 size reached 100~200 mm³, mice were treated orally with saline, erlotinib (50 mg/kg),
179 phlorizin (20 mg/kg), LX4211 (60 mg/kg), or the indicated combination for 30 days.
180 A549/Luc cells were intravenously injected into the SCID mice. Tumor volume, as
181 indicated by luciferase intensity, was measured by the Lumina LT In Vivo Imaging
182 System (IVIS; PerkinElmer Inc., Waltham, MA, USA).

183

184 ***Site-directed mutagenesis***

185 The human EGFR T678A, EGFR S1046/47AA mutants were generated by using the
186 QuikChange Site-Directed Mutagenesis kit (Agilent Technologies Inc., Santa Clara,

187 CA, USA) following the manufacturer's protocol. The primers were listed in the
188 Supplementary information. Each mutation was verified by DNA sequencing.

189

190 ***Transient Transfection***

191 Cells with 80% of confluence were subjected to transfection by incubation with
192 DNA/TransIT[®]-X-2 (Mirus Bio, Madison, WI, USA) complex (ratio of 1:1.2) in
193 serum-free medium for 6 hours followed by the refreshment with complete medium.
194 The cells were harvested and subjected to the experiments after 72 hours of
195 transfection.

196

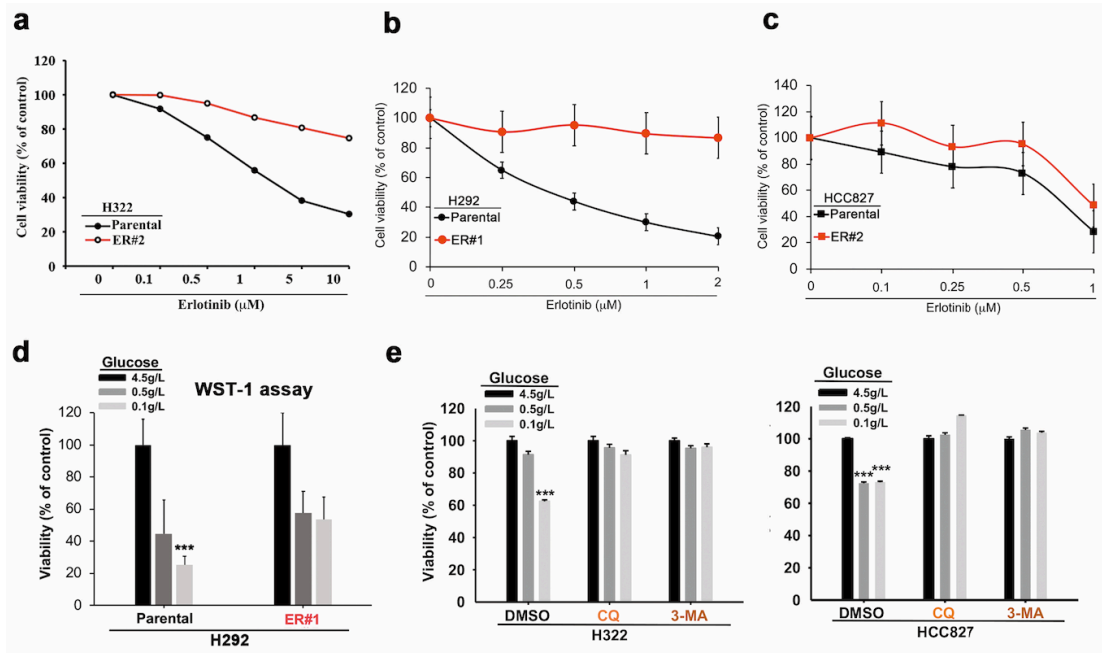
197 ***Gene silence with shRNA***

198 The shRNA clones against the indicated human genes were purchased from the
199 National RNAi Core Facility at Academia Sinica (Taipei, Taiwan). Briefly, cells were
200 infected with the indicated viral shRNA at the multiplicity of infection (MOI) of 125
201 for 3 days. Cells were refreshed with complete medium and then further subjected to
202 the indicated experiments.

203

204 ***Statistical analysis***

205 Analyses of patient survival and progression-free rates were performed using
206 GraphPad Prism 8. Other statistical analysis was performed by Sigma plot. Data are
207 displayed as the means \pm SEM. The significance of the difference between the
208 experimental and control groups was assessed by Student's *t*-test. The difference was
209 considered to be significant if the *P*-value was < 0.05 .



210

211 **Supplementary Fig S1. The acquired erlotinib-resistant NSCLC cells were more**

212 **tolerant to glucose deprivation. a-c.** H322, H292, and HCC827 cells and their ER

213 clones were treated with different concentrations of erlotinib. The viability was

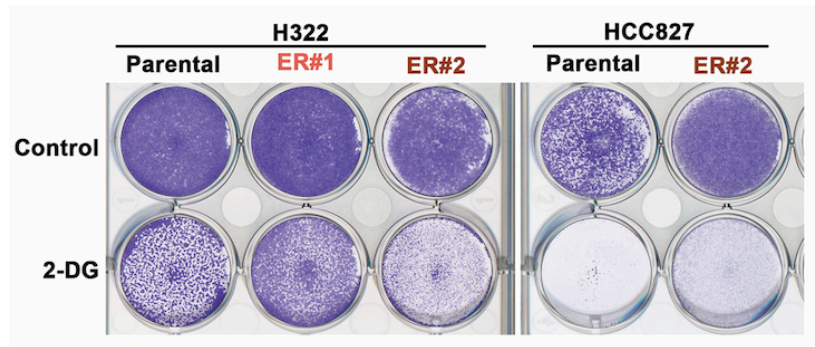
214 determined by MTT assay. **d.** H292 cells and their ER clone were cultured in different

215 concentrations of glucose. The cell viability was measured in MTT. **e.** The effects of

216 3-MA or CQ on the glucose deprivation-induced cell death were examined in WST-1

217 analysis. Data in **(a-e)** represent as mean±s.d. from three independent experiments. **P*

218 < 0.05; ****P*< 0.001 vs control group, Student's t test.

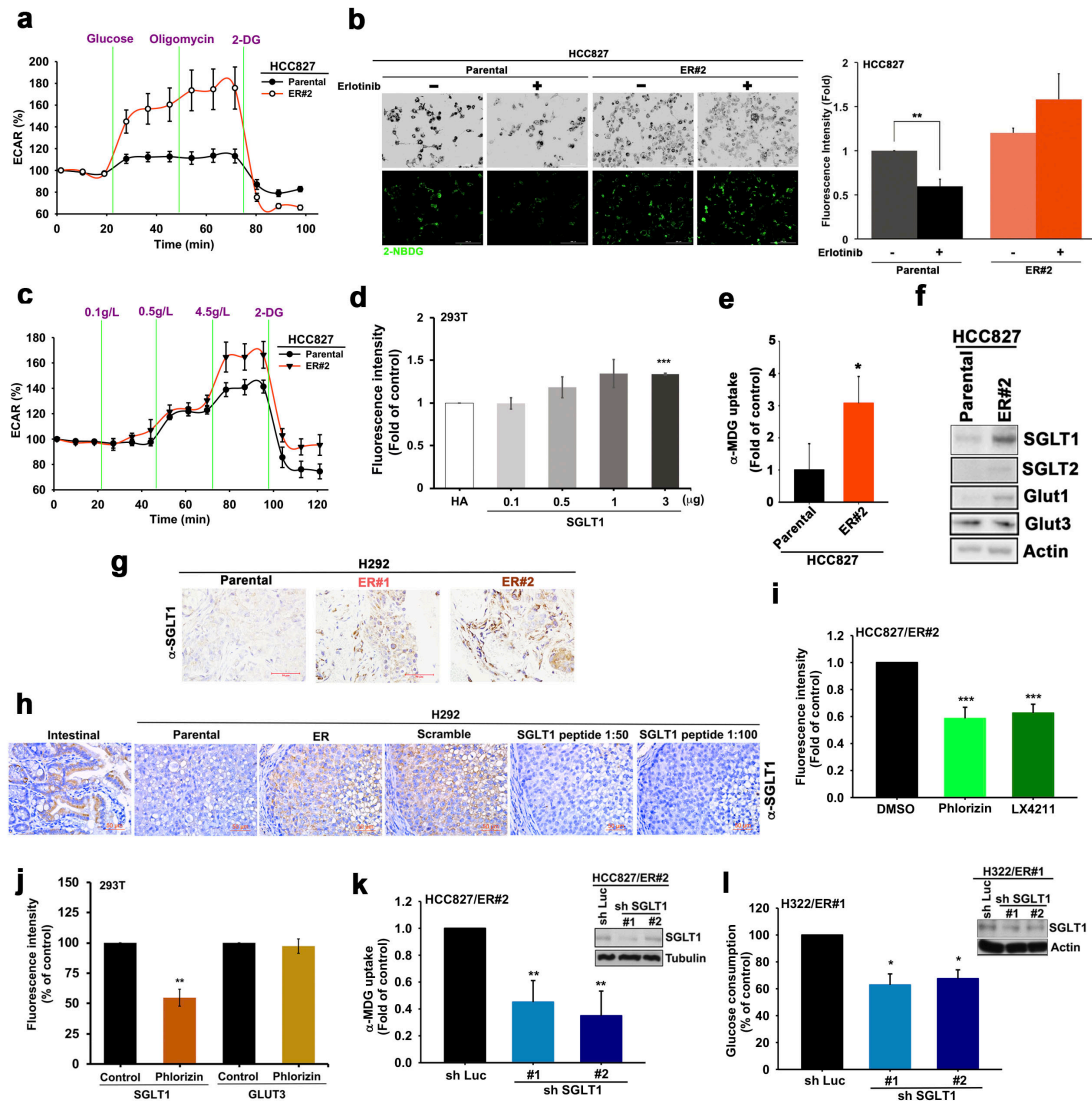


219

220 **Supplementary Fig S2. Block of glycolysis decreased cell growth.**

221 The inhibitory effects of 2-DG on the viability in H322 and HCC827 cells and their

222 ER clones were measured by clonogenic assay.



223

224 **Supplementary Fig S3. The upregulated SGLT1 mediated glucose uptake of the**

225 **acquired erlotinib-resistant cells. a.** Changes in ECAR of HCC827 and their ER

226 clones were measured by using the XF-24 Seahorse extracellular flux analyzer. **b.**

227 2-NBDG uptake ability of HCC827 and its ER clones under EGFR-TKI treatment

228 were detected by immunofluorescent. Scale bar, 200 μm. **c.** Changes in ECAR in

229 HCC827 and its ER clones in response to different glucose concentrations treatment

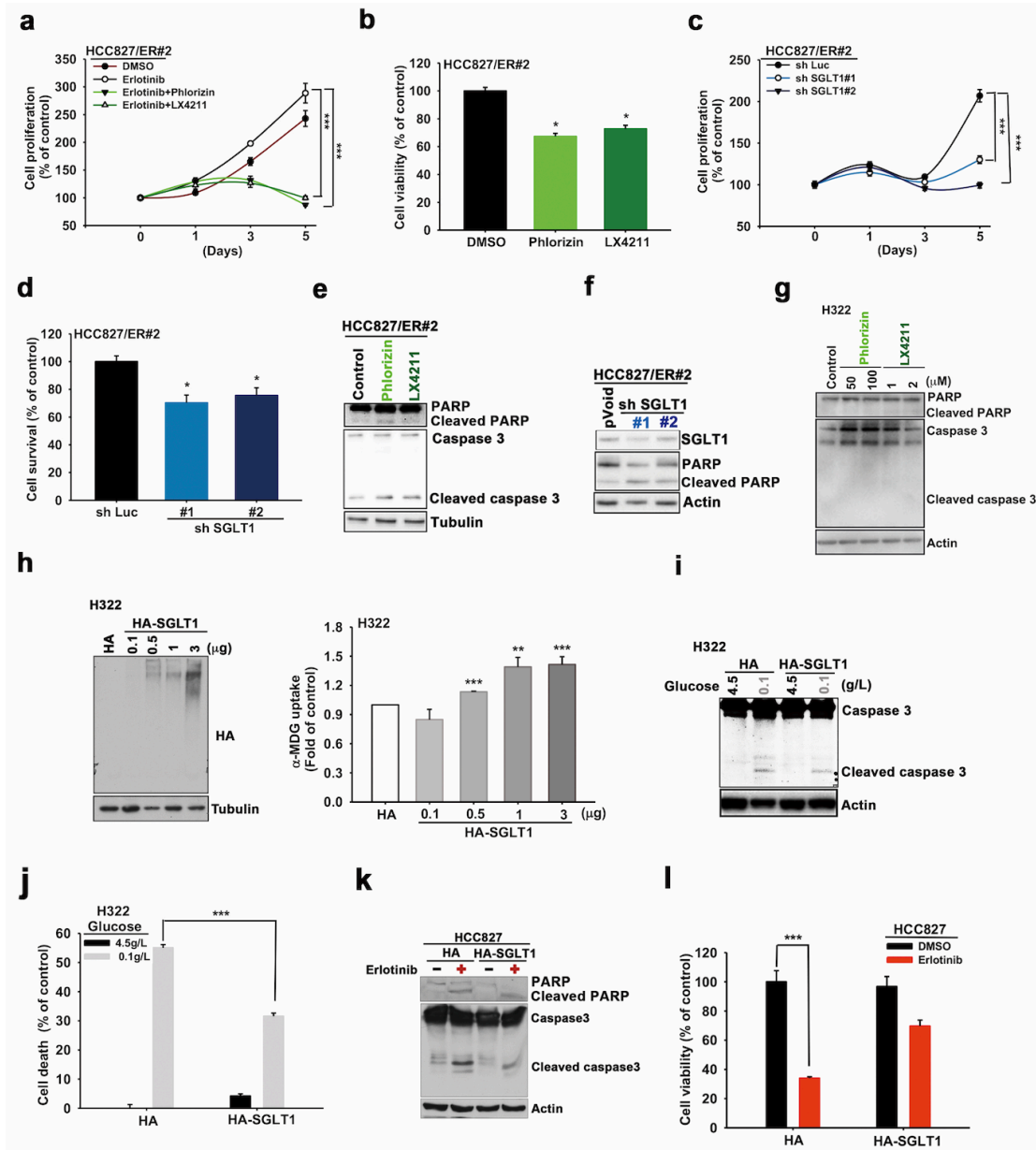
230 were analyzed in XF-24 Seahorse extracellular flux analyzer. **d.** HEK-293T cells

231 transfected with increasing amounts of SGLT1 cDNA were subjected to 2-NBDG

232 uptake analysis. **e.** α-MDG uptake ability of HCC827 cells and their ER clones was

233 detected by FACS and Beckman LS6000 Scintillation Counter. **f.** Protein levels of the

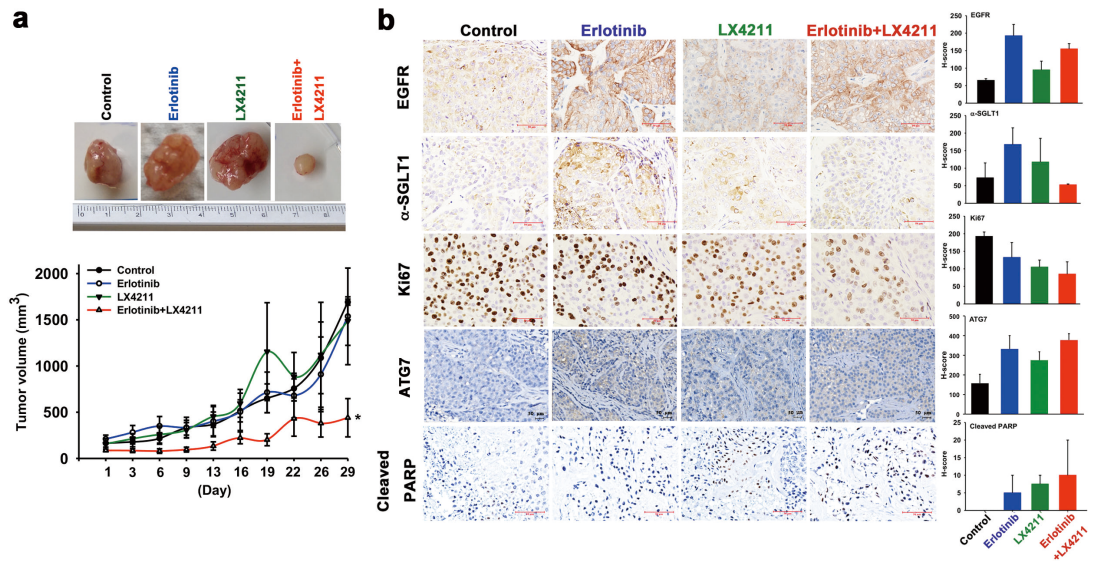
234 indicated glucose transporters in HCC827 and its ER clone cells were detected in WB
235 with the indicted antibodies. **g and h.** Representative images of IHC staining of
236 SGLT1 expression in the tumor sections from H292 and H292/ER cells (**g**) by using
237 the specific anti-SGLT1 antibody which was validated with competitive peptide
238 corresponding to the epitope sequence of SGLT1 (a.a.601-630) (**h**). Scale bar, 50 μ m.
239 **i.** The effects of 100 μ M phlorizin or 1 μ M LX4211 on 2-NBDG uptake ability in
240 HCC827/ER#2 clones under a low glucose concentration condition were examined. **j.**
241 The effects of phlorizin on 2-NBDG uptake ability of SGLT1- or Glut3-transfected
242 HEK-293T cells under a low glucose concentration condition were examined. **k.** The
243 effects of SGLT1 shRNA on the α -MDG uptake ability of HCC827/ER#2 clone were
244 measured under low glucose condition by using Beckman LS6000 Scintillation
245 Counter. **l.** The effects of SGLT1 shRNA on glucose consumption level of
246 H322/ER#1 clone were analyzed. Data shown in (**a**), and (**c-e**), and (**i-l**) represent as
247 mean \pm s.d. from three independent experiments. * $P < 0.05$; ** <0.01 ; *** $P < 0.001$ vs
248 control group, Student's t test. Data in (**b**), (**g**) and (**h**) are representative of three
249 experiments.



250

251 **Supplementary Fig S4. The upregulated SGLT1 supported the cell viability of**
 252 **the acquired TKI-resistant cells. a.** The cell proliferation of HCC827/ER clones in
 253 response to erlotinib, phlorizin, or LX4211 were determined in WST-1 analysis. **b.**
 254 The effects of phlorizin or LX4211 on cell viability of HCC827/ER#2 clones under
 255 low glucose concentration were measured in WST-1 analysis. **c and d.** The effects of
 256 SGLT1 shRNA on cell proliferation (c) and viability (d) of HCC827/ER#2 clones
 257 under low glucose concentration were determined in cell counting and WST-1
 258 analyses, respectively. **e and f.** The effects of SGLT1 inhibitors (e) and shRNA (f) on

259 PARP cleavages, caspase 3 in HCC827/ER#2 clones were analyzed by WB. **g.** The
260 effects of SGLT1 inhibitors on PARP cleavages, caspase 3 in H322 cells were
261 analyzed by WB. **h.** H322 cells transfected with different amounts of SGLT1 cDNA
262 were subjected to analyze the SGLT1 protein level in WB (left) and to measure
263 α -MDG uptake (right). **i.** The effects of SGLT1 overexpression on caspase 3 cleavage
264 induced by glucose deprivation in H322 cells were analyzed by WB. **j.** The relative
265 cell death of SGLT1-expressing H322 cells in response to glucose deprivation was
266 measured in WST-1 analysis. **k and l.** The effects of SGLT1 overexpression on the
267 erlotinib-induced PARP and caspase 3 cleavages (**k**) and cell death (**l**) in HCC827
268 cells were analyzed in WB and WST-1 analyses, respectively. Data in **(a-d)**, **(h)**, and
269 **(j)** represent the mean and s.d. from three independent experiments. * $p < 0.05$; *** $p <$
270 0.001 vs control group, Student's t test. Data in **(e-g)**, **(i)** and **(k)** are representative of
271 three experiments.



272

273 **Supplementary Fig S5. Targeting SGLT1 reduced the development of acquired**

274 **resistance to EGFR TKI *in vivo*.** **a.** The growth rate of xenograft tumors of H292

275 cells in response to treatments with erlotinib, LX4211, or the combination of erlotinib

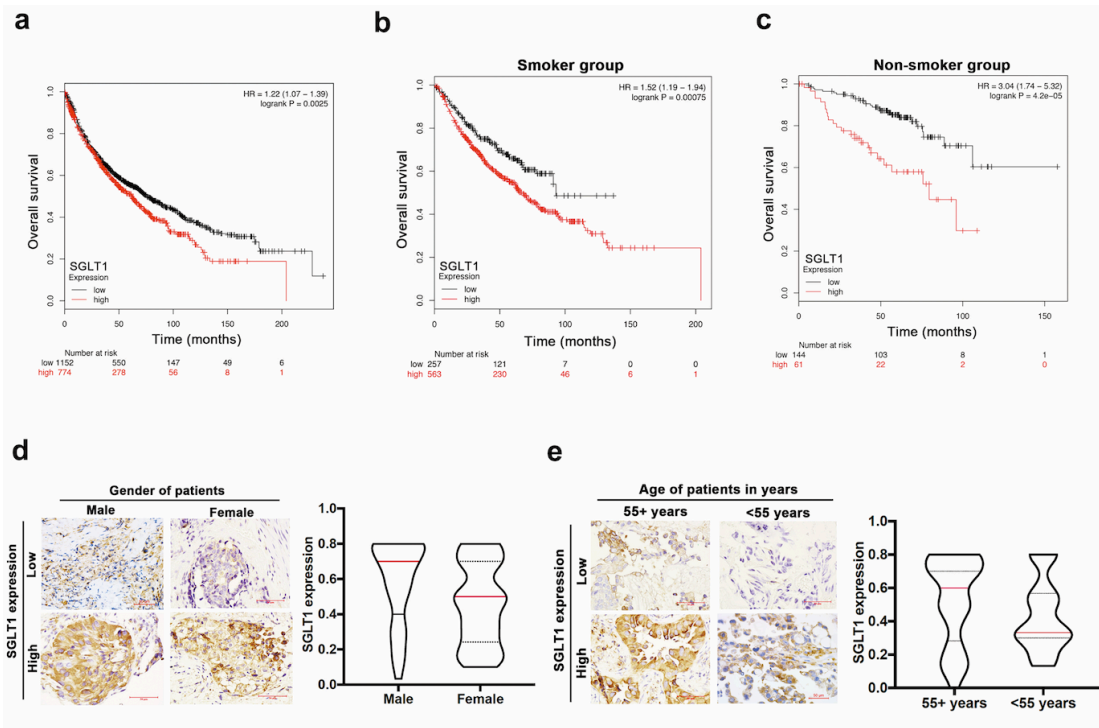
276 and LX4211 was determined by measuring the tumor size. **b.** Representative IHC

277 staining of xenograft tumors from (a) was performed with the indicated antibodies,

278 and the H-score of protein expression was shown. Scale bar, 50 μm. Data represent

279 mean±s.d. * $p < 0.05$ vs control group, Student's t test.

280



281

282 **Supplementary Fig S6. SGLT1 expression negatively correlates with the clinical**

283 **benefits of EGFR TKI in NSCLC patients. a.** The clinical correlation of SGLT1

284 mRNA expression with overall survival rate was analyzed in the Kaplan Meier

285 analysis. **b, c.** The SGLT1 mRNA expression was further classified into with (b) and

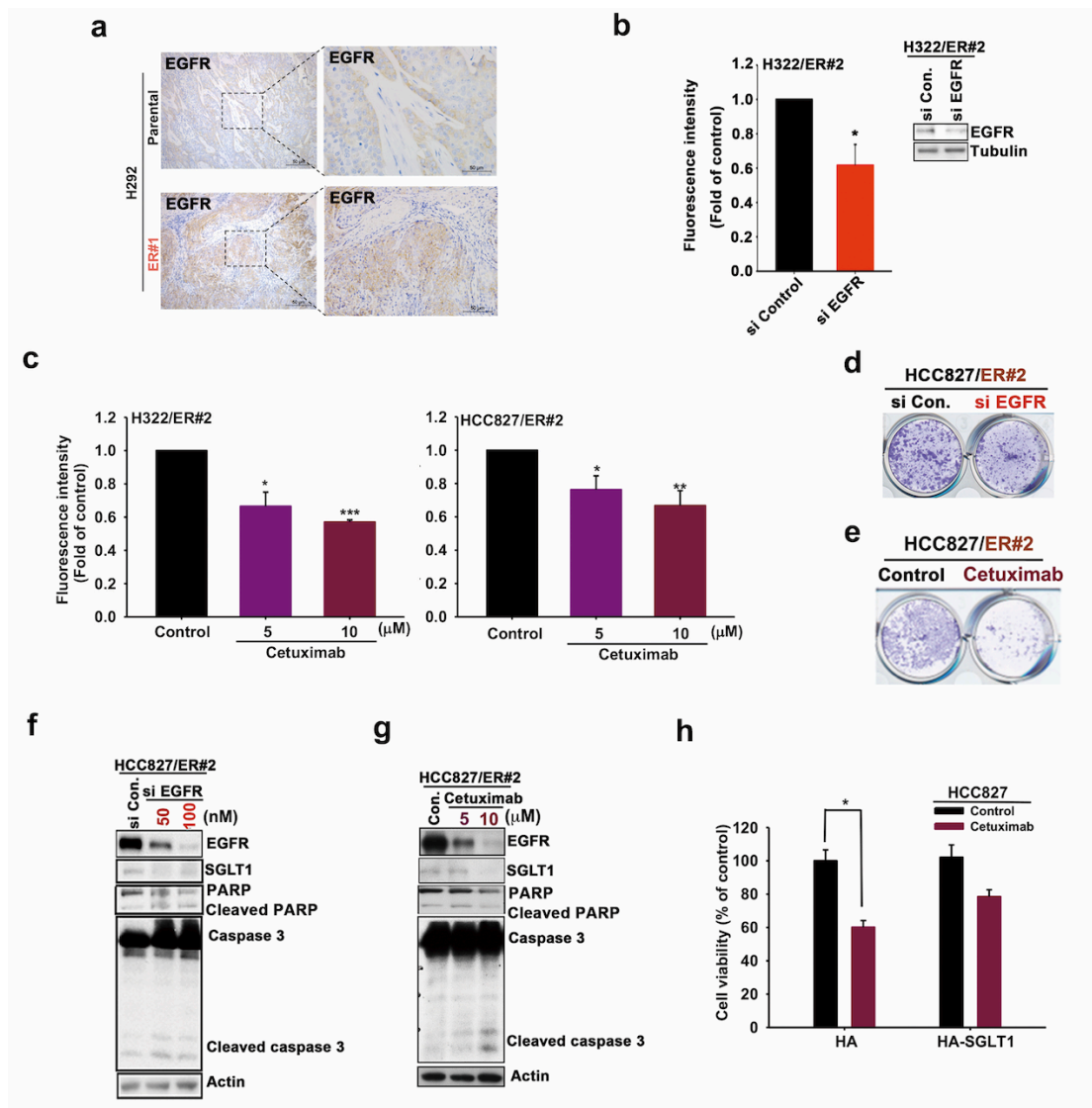
286 without cigarette smoke (c) groups for Kaplan-Meier overall survival. **d, e.** The

287 SGLT1 protein level in the paired tissues from treatment-naïve tumors and acquired

288 TKI-resistant tumors of 9 lung cancer patients were examined by IHC staining and

289 quantitated. The representative data was shown according to the gender (d) and age

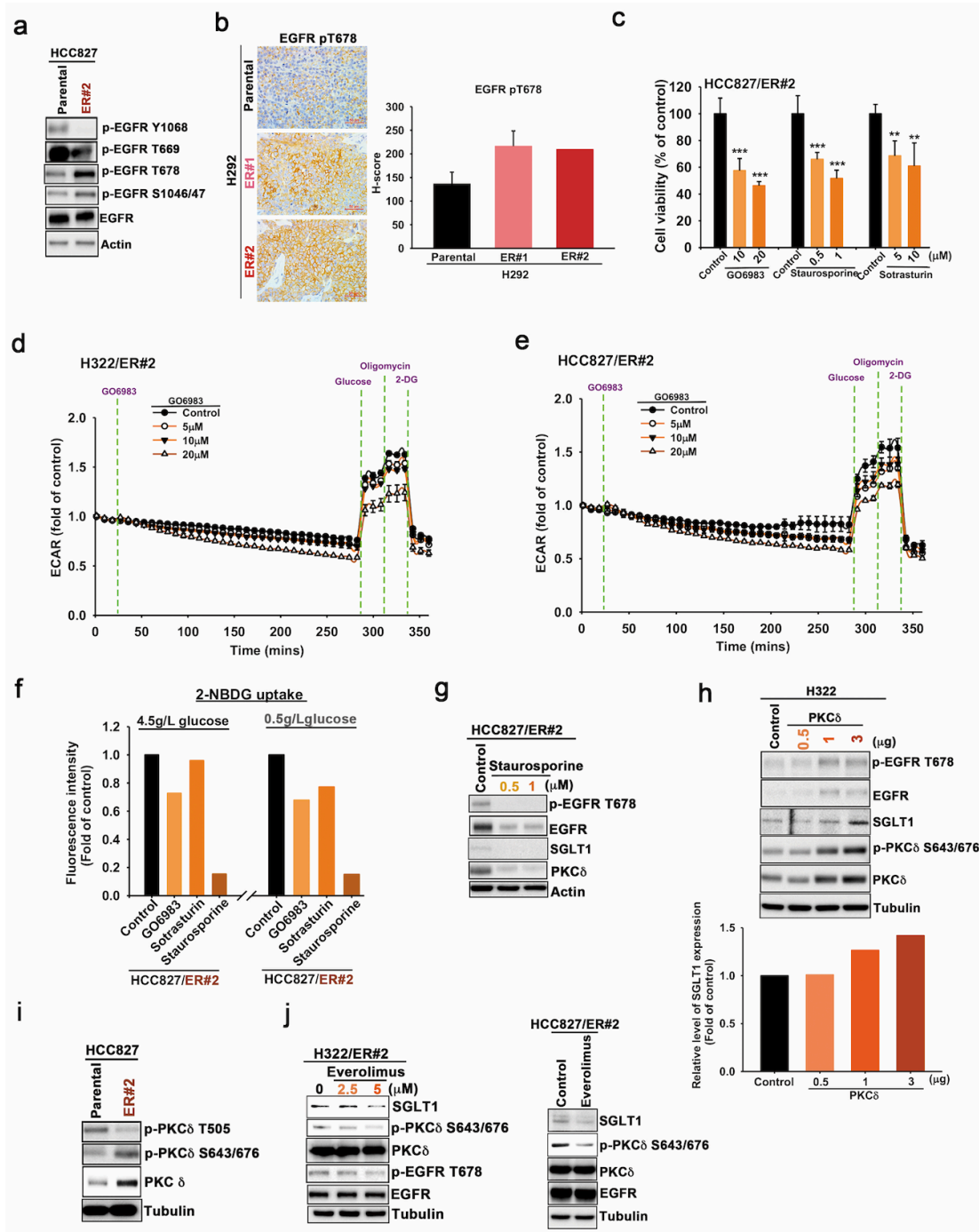
290 (e). Scale bar, 50 μ m.



291

292 **Supplementary Fig S7. The increased EGFR mediated the glucose uptake and**
 293 **viability of the acquired erlotinib-resistant cells through SGLT1 upregulation. a.**
 294 The EGFR protein staining of H292 cells-xenograft tumor sections in response to
 295 erlotinib treatment was performed in IHC analysis. Scale bar, 50μm. **b-g.** The effects
 296 of monoclonal antibody cetuximab or EGFR siRNA on 2-NBDG uptake (b and c),
 297 colony formation (d and e), and caspase and PARP cleavages (f and g) of
 298 HCC827/ER#2 cells were determined, respectively. **h.** The effects of SGLT1
 299 overexpression on the cetuximab-induced viability inhibition of HCC827 cells were
 300 examined in WST-1 analysis. Data in (b and c), and (h) represent as mean±s.d. from
 301 three independent experiments. * $p < 0.05$; ** $p < 0.01$; *** $p < 0.001$ vs control group,

302 Student's t test. Data in **(a)** and **(d-g)** were representative of three experiments.



303

304 **Supplementary Fig S8. EGFR Thr678 phosphorylation by PKC delta mediated**
 305 **the SGLT1/EGFR interaction for SGLT1 protein stabilization.** a. The protein and
 306 phosphorylations of EGFR in HCC827 cells and their ER clones were analyzed in
 307 WB analysis. b. Representative IHC image and H-score of EGFR p-T678 expression
 308 in xenograft tumor sections of H292 cells and their ER clones were shown. Scale bar,
 309 50 μ m. c. The effects of GO6983, staurosporine, sotrasturin or HBDDE on cell

310 viability were determined in WST-1 assay. **d, e.** Changes in ECAR in H322/ER#2 (d)
311 and HCC827/ER#2 (e) cells in response to GO6983 treatment for 4 hrs were analyzed
312 in XF-24 Seahorse extracellular flux analyzer. **f.** The effects of various PKC
313 inhibitors treatment on 2-NBDG uptake ability were analyzed by FACS analysis. **g-j.**
314 The total lysates from staurosporine-treated HCC827/ER#2 cells (g),
315 PKC δ -transfected H322 cells (h), HCC827 cells and their ER clones (i), and
316 everolimus-treated H322/ER#2 cells (j) were subjected to WB analysis with the
317 indicated antibodies. Data shown in **(c)**, **(d)**, and **(e-f)** represent as mean \pm s.d. from
318 three independent experiments. *** $p < 0.001$ as compared with control group using
319 Student's t test. Data in **(a)**, **(b)**, and **(g-j)** were representative of three experiments.

320 Table 1. Association of SGLT1 with clinical characteristics

		Analysis patients' number	SGLT1		p value
			High	Low	
		Total number (72)			
Gender					
	Male	35	18 (51.4%)	17 (48.5)	0.018*
	Female	37	9 (24.3%)	28 (75.6)	
Age (years)					
	≥55	53	26 (49.0%)	27 (50.9%)	0.003**
	<55	19	2 (10.5%)	17 (89.4%)	
Smoke					
	Smoker	26	12 (46.1%)	14 (53.8%)	0.254
	Non-smoker	46	15 (32.6%)	31 (67.3%)	
EGFR status					
	WT	33	9 (27.2%)	24 (72.7%)	0.099
	Mutation	39	18 (46.1%)	21 (53.8%)	
	del.19	20	10 (50%)	10 (50%)	
	L858R	16	7 (43.7%)	9 (56.2%)	
	del.19/T790M	1	0 (0%)	1 (100%)	
	L816Q	1	1 (100%)	0 (0%)	
	exon 20	1	0 (0%)	1 (100%)	
					0.552
Clinical T-stage					
	Tx-T0	5	2 (40%)	3 (60%)	0.662
	T1-T2	14	7 (50%)	7 (50%)	
	T3-T4	44	16 (36.3%)	28 (63.6%)	
Clinical N-stage					
	x	4	2 (50%)	2 (50%)	0.37
	0	11	6 (54.5%)	5 (45.4%)	
	1	3	0 (0%)	3 (100%)	
	2	20	9 (45%)	11 (55%)	
	3	26	8 (30.7%)	18 (69.2%)	
Pathological staging (AJCC)					
	Stage I	0	0 (0%)	0 (0%)	0.081
	Stage II	1	1 (100%)	0 (0%)	
	Stage III	5	0 (0%)	5 (100%)	
	Stage IV	44	19 (43.1%)	25 (56.8%)	
TKI drug therapy					
	Gefitinib	36	16 (44.4%)	20 (55.5%)	
	Erlotinib	35	13 (37.1%)	22 (62.8%)	

	Afatinib	2	0 (0%)	2 (100%)	0.417
TKI response CT					
	PR	20	8 (40%)	12 (60%)	
	SD	9	3 (33.3%)	6 (66.6%)	
	PD	38	16 (42.1%)	22 (57.8%)	0.89

321 * $P < 0.05$ and * $P < 0.01$